Tuning Optical Properties of Magic Number Cluster $(SiO_2)_4O_2H_4$ by Substitutional Bonding with Gold Atoms

Xiulong Cai,[†] Peng Zhang,[†] Liuxue Ma,[†] Wenxian Zhang,[†] Xijing Ning,[‡] Li Zhao,[§] and Jun Zhuang*,[†]

Department of Optical Science and Engineering, State Key Laboratory for Advanced Photonic Materials and Devices, Institute of Modern Physics, Department of Physics, Fudan University, Shanghai 200433, China

Received: December 23, 2008; Revised Manuscript Received: March 11, 2009

By bonding gold atoms to the magic number cluster $(SiO_2)_4O_2H_4$, two groups of Au-adsorbed shell-like clusters $Au_n(SiO_2)_4O_2H_{4-n}$ ($n = 1-4$) and $Au_n(SiO_2)_4O_2$ ($n = 5-8$) were obtained, and their spectral properties were studied. The ground-state structures of these clusters were optimized by density functional theory, and the results show that in despite of the different numbers and types of the adsorbed Au atoms, the cluster core $(SiO_2)_4O_2$ of T_d point-group symmetry keeps almost unchanged. The absorption spectra were obtained by time-dependent density functional theory. From one group to the other, an extension of absorption wavelength from the UV−visible to the NIR region was observed, and in each group the absorption strengths vary linearly with the number of Au atoms. These features indicate their advantages for exploring novel materials with easily controlled tunable optical properties. Furthermore, due to the weak electronic charge transfer between the Au atoms, the clusters containing Au_2 dimers, especially $Au_8(SiO_2)_4O_2$, absorb strongly NIR light at 900∼1200 nm. Such strong absorption suggests potential applications of these shell-like clusters in tumor cells thermal therapy, like the gold-coated silica nanoshells with larger sizes.

Introduction

Nanomaterials have always attracted scientists' interest due to their unique physical and chemical properties compared with their bulk counterparts and have induced many novel applications in a wide range of fields. Gold, one of the noble metals, has been extensively studied not only in chemistry and physics but also in biology and medicine, because of the noncytotoxicity and biocompatibility of its nanoparticles.[1,2] In particular, gold nanoparticles, such as nanospheres and nanorods, show great potential in cancer diagnosis and therapy, because they have strong surface-plasmon-resonance (SPR) enhanced light scattering and absorption.[1,3−5] Recently, the gold-coated silica nanoshells became particularly attractive for the photothermal therapy of cancer cells and have been demonstrated effective agents experimentally in vitro and in vivo with mice.[6,7] For in vivo therapy application, the nanomaterials are required to intensively absorb the near-infrared (NIR, 600∼1300 nm) light, since light in this region has the highest transmissivity in human tissues.[8,9] By varying the ratio of the shell thickness with respect to the diameter of the core, it is easy to tune the optical resonance wavelength of silica-gold nanoshells within a broad range extended from the visible to the NIR region.[10] The tunability originates from the interaction of the plasmons on the inner and outer surfaces of the gold shells.[11]

However, nanoshells are usually so large (about 100∼400 nm in diameter) that their transvascular transport may be limited in some tumors.[12] Smaller size particles can be transferred more easily in the live tissues and be delivered more effectively to target cells. Therefore, clusters in molecular scale (of the order of 1 nm) will be more promising if they also behave like the nano ones in the NIR region. Recently, as such small-size materials, Au-adsorbed $(SiO_2)_3$ and Ag-adsorbed $(SiO_2)_n$ ($n = 1-7$) clusters were considered theoretically by Sun et al.[13] and Zhao et al.,[14] respectively. On the other hand, magic number clusters, owing to their highly symmetric geometries and outstanding stabilities, are also of great interest for exploring novel materials with tunable optical properties by doping or decorating, such as C_{60} and Au_{20}.[15,16] In the present work, based on the magic number cluster $(SiO_2)_4O_2H_4$ discovered in our previous works,[17,18] two groups of small shell-like clusters in molecular scale $Au_n(SiO_2)_4O_2H_{4-n}$ ($n = 1-4$) and $Au_n(SiO_2)_4O_2$ ($n = 5-8$) as the counterparts of the large gold-coated semicontinuous nanoshells were constructed and studied theoretically, including their ground-state structures and optical properties. The cluster structures constructed here are similar to those of the gold adsorbed defect model Au-$(Si_5O_9H_7)$ and Au_2-$(Si_5O_9H_7)$ discussed recently in the experiments of gold atoms adsorbing on silica surface.[19,20] In the following sections, we will describe the cluster models and the computational approaches employed in this work, as well as the detailed results and discussions. It is shown that owing to the outstanding stability of the core of the shell-like clusters, the optical absorption spectra of these clusters can be tuned effectively and definitely by changing the types and the number of the gold adsorbates.

Cluster Models and Computational Details

In our previous XeCl excimer laser (308 nm) ablation experiments of porous siliceous materials, a series of SiO_2-based clusters have been generated efficiently, and what attracted our particular attention is the observation of the magic number clusters $[(SiO_2)_4O_2H_3]^-$ and $[(SiO_2)_8O_2H_3]^-$ in the mass spectra. For clusters, as we know, "magic" means high natural abun-

* To whom correspondence should be addressed. E-mail: zhuang1022@gmail.com.
[†] Department of Optical Science and Engineering, State Key Laboratory for Advanced Photonic Materials and Devices.
[‡] Institute of Modern Physics.
[§] Department of Physics.

10.1021/jp811347c CCC: $40.75
Published on Web 04/08/2009

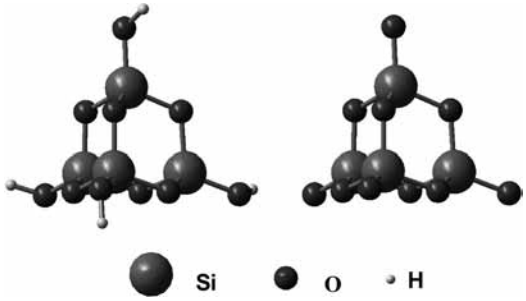

Figure 1. Ground-state structures of the magic number cluster $(SiO_2)_4O_2H_4$ (left) and its core $(SiO_2)_4O_2$ (right). The cluster $(SiO_2)_4O_2H_4$ is of S_4 point-group symmetry and the core $(SiO_2)_4O_2$ is of T_d symmetry.

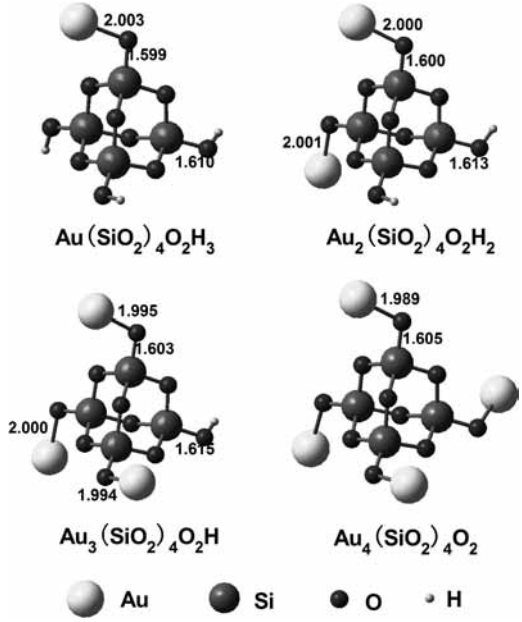

Figure 2. Ground-state structures of Au_1-adsorbed clusters $Au_n(SiO_2)_4O_2H_{4-n}$ ($n = 1-4$). Calculated bond lengths are given in angstroms.

dance, structural stability, and mass-preparation possibility. An attractive potential application of magic number clusters is the use as building blocks for new cluster materials. Combining genetic algorithm and density functional theory (DFT), we found that the ground state of the neutral $(SiO_2)_4O_2H_4$ cluster has a pseudotetrahedral structure of S_4 point-group symmetry,[18] in which the skeleton $(SiO_2)_4O_2$ is an oxy-silica cluster of tetrahedral T_d symmetry (Figure 1). Moreover, this oxy-silica cluster plays a key role in the magic behavior of $(SiO_2)_4O_2H_4$, while the terminal hydrogen atoms are just for saturating the dangling oxygen atoms. These features motivated our interest in substituting gold atoms for hydrogen ones in the magic number cluster for constructing small shell-like clusters with tunable optical properties. Through a sequence of replacement, gold monatomic and diatomic adsorptions to the oxygen atoms of $(SiO_2)_4O_2$ were considered sequentially as shown in Figures 2 and 5, which would perform as a process of gold growing on $(SiO_2)_4O_2$ as well. These gold-substituted models could be supported by the recent experiments of gold atoms depositing on amorphous silica surface, where clusters Au-$(Si_5O_9H_7)$ and Au_2-$(Si_5O_9H_7)$ similar to our clusters were used to model the gold adsorbed defects.[19,20] Furthermore, it was concluded in those studies that single gold atoms or gold dimers are preferentially bound to the dangling oxygen defects, providing reliability for our constructed clusters with gold atoms or dimers

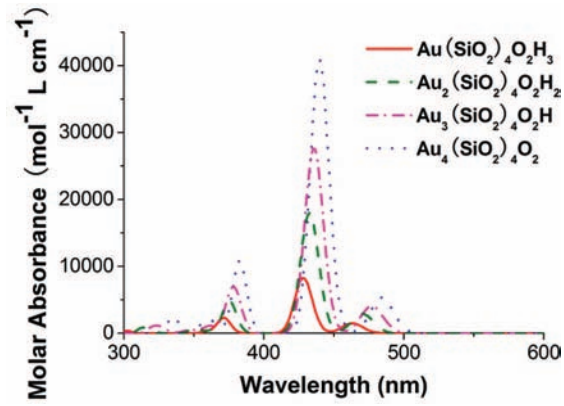

Figure 3. Absorption spectra of clusters $Au_n(SiO_2)_4O_2H_{4-n}$ ($n = 1-4$) calculated with TDDFT/B3PW91 method. The spectra are broadened with a Guassian type of width 0.1 eV.

adhering to oxygen atoms. From the structures shown in Figures 2 and 5, it is natural that we can draw analogies between the cluster skeleton $(SiO_2)_4O_2$ and the nanosize silica core, as well as between the gold atoms adsorbed outside $(SiO_2)_4O_2$ and the semicontinuous gold shell, respectively.

To study the optical properties of these shell-like clusters, we used the static DFT method to determine their ground-state structures and the time-dependent DFT (TD-DFT) approach to calculate the vertical excitation energies. TD-DFT is one of the powerful methods to study the photoabsorption properties of small systems, including gold clusters and gold compounds.[13,21-23] All of our calculations were performed with the Gaussian 03 program.[24] When a series of vertical excitation energies and corresponding oscillator strengths are determined, the molar absorbance related to photon energy can be obtained with the following expression

$$\varepsilon(\omega) = c\sum_I \frac{f_I}{\Delta_{1/2,I}} \exp\left(-2.773\frac{(\omega-\omega_I)^2}{\Delta_{1/2,I}^2}\right)$$

where f_I is the oscillator strength corresponding to the vertical excitation energy ω_I, $\Delta_{1/2,I}$ is the half-bandwidth, and c is a constant. These spectra calculations were implemented by the SWizard program.[25]

In this work, the structural optimizations and excitation calculations were implemented in the same theoretical level. It is well known that TD-DFT results are usually sensitive to the choice of the exchange-correlation functionals. Thus, it is necessary to make comparisons of different theoretical models and choose a relatively more accurate one. For this purpose, we calculated the vertical excitation energies of the AuO cluster with different exchange-correlation functionals and basis sets, and then compared these results with others' work.[26] The reason is that AuO radicals are the terminals of our first group clusters and play important roles in the absorption spectra, which will be illustrated below. In the comparisons, we found that the basis sets just made negligible influences on the spectra but the general gradient approximate (GGA) functional and the hybrid functional produced different results. With the same mixed basis sets (6-311++G(3df,3pd) for Si, O, and H atoms and a relativistic effective core potential (ECP) basis set for Au atoms[27]), we optimized the structure and calculated the excitation energies of AuO cluster using PW91PW91 and B3PW91 functionals, respectively. We got the excitation energy of the second dipole-allowed transition $X^2\Pi \rightarrow A^2\Sigma^+$ of 1.271 eV with the first model and 1.545 eV with the second. Compared to the

TABLE 1: Calculated Excitation Energies (E, eV), Wavelengths (λ, nm), and Corresponding Oscillator Strengths (f) of $Au_n(SiO_2)_4O_2H_{4-n}$ ($n = 1-4$) Clusters in the Visible Region[a]

	$Au(SiO_2)_4O_2H_3$			$Au_2(SiO_2)_4O_2H_2$			$Au_3(SiO_2)_4O_2H$			$Au_4(SiO_2)_4O_2$		
range	E	λ	$f \times 100$	E	λ	$f \times 100$	E	λ	$f \times 100$	E	λ	$f \times 100$
450−500 nm	2.68	463.1	0.56	2.63	470.8	0.56	2.59	478.5	0.57	2.56	484.5	0.49
				2.64	469.6	0.54	2.60	477.6	0.45	2.56	484.5	0.49
							2.61	474.9	0.53	2.56	483.8	1.02
400−450 nm	2.90	428.1	3.08	2.86	433.1	4.98	2.84	436.5	3.36	2.82	439.7	7.45
				2.88	430.9	1.80	2.85	435.7	6.15	2.82	439.5	3.90
										2.82	439.5	3.90

[a] The first row gives the optical gaps of these clusters.

value of 1.785 eV calculated by O'Brien,[26] the hybrid functional gives a more accurate result than the GGA method for our system. Thus, the hybrid B3PW91 functional with the mixed basis sets referred above was adopted in our whole calculations. In addition, the magic number cluster $(SiO_2)_4O_2H_4$ is a reasonable model for hydroxylated silica surface,[28] and the cluster core $(SiO_2)_4O_2$ behaves as an oxygen defect model of silica surface like $Si_5O_9H_7$. It is then reasonable to compare our calculated spectra of the clusters with the experimental measurements of silica surface. In the following sections, we will see the accordance between our calculations and the measurements by Antonietti et al.,[19,20] which indicates that our calculations with the functional and basis sets selected above are reliable.

In our studies, we considered two steps in the process of gold atom growth on the core $(SiO_2)_4O_2$, first single Au atoms being substituted for hydrogen atoms and then continuing to form Au_2 dimers. According to this process, we classified our concerned shell-like clusters into two groups: one is Au_1-adsorbed group whose members contain only single Au atoms in the terminal sites, and the other is Au_2-adsorbed group which includes those clusters with Au_2 dimers combined to the dangling O atoms. Since this is a gold-substituted process, the geometry optimizations of these clusters were carried out starting from the configuration of $(SiO_2)_4O_2H_4$ in the selected theoretical level and the vibrational frequencies of the optimized clusters were calculated to confirm that they have reached the local minima of the potential energy surfaces. In the optimizations, no symmetric constraints were used in the optimization processes, so it is reasonable to consider these optimized structures as the natural results of gold growth. Finally, a series of vertical excitation energies of each cluster were computed with TD-DFT method and the corresponding absorption spectrum was obtained.

Results and Discussions

1. Clusters with Single Au Atoms at Terminals ($n = 1-4$). The Au_1-adsorbed cluster group in which only single Au atoms are coordinated with the dangling O atoms is considered first. In this case, when the substituted number of gold atoms n is less than 4, there still exist hydroxyl radicals where the hydrogen atoms perform a role in saturating the oxygen ones like in the original cluster $(SiO_2)_4O_2H_4$. Thus, for this group we use $Au_n(SiO_2)_4O_2H_{4-n}$ ($n = 1-4$) to represent the clusters, and Figure 2 shows their equilibrium structures in the ground states. Because the Au atom has an unpaired 6s electron, it can be coordinated to O atom just like H atom. Therefore, in this group all atoms are fully coordinated and all electrons must be spin paired so the spin multiplicities of these Au_1-adsorbed clusters are singlet in their ground states. According to the optimized results, in each cluster with different number n, the cluster core $(SiO_2)_4O_2$ always approximately maintains T_d point-group symmetry with trivial changes in its bond lengths and bond angles. This result indicates a corelike behavior and is within our expectation because of the outstanding structural stability of the magic number cluster. The clusters $Au_n(SiO_2)_4O_2H_{4-n}$ ($n = 1-4$) also display slight differences in Au−O bond lengths and Au−O−Si bond angles. As gold atoms increase, the Au−O bond lengths only decrease from 2.003 to 1.989 Å and the Au−O−Si bond angles vary in the range from 114 to 118°. We also carried out the geometry optimization of the gold monoxide AuO in the same theoretical level and found the bond distance about 1.909 Å, which is in good agreement with the other theoretical result of 1.907 Å[29] and experimental finding of 1.849 Å.[30] Therefore, the bond lengths of the AuO radicals in these clusters are about 0.1 Å larger than that of its diatomic compound. These extensions of bond lengths, reflecting the weakening of interactions between Au and O atoms, result from the decrement of electron-cloud densities of Au−O bonds in the Au_1-adsorbed clusters, because partial electrons of the O atoms should shift toward the Si atoms to form the O−Si covalent bonds.

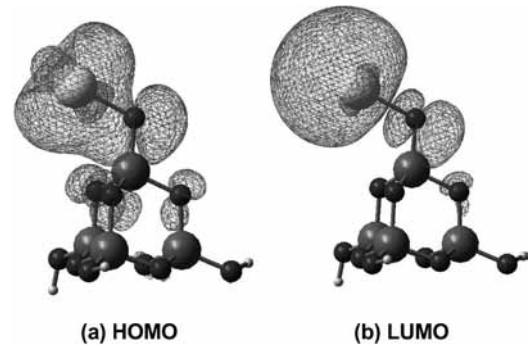

Figure 4. The HOMO and LUMO orbitals of the cluster $Au(SiO_2)_4O_2H_3$.

On the basis of the optimized configurations of these clusters, we calculated their vertical excitation energies and analyzed the absorption spectra. In order to study how the Au atoms modify the optical properties of the clusters, the absorption properties of the original cluster $(SiO_2)_4O_2H_4$ was also calculated and compared with the Au_1-adsorbed ones. The results of our calculations show that the cluster $(SiO_2)_4O_2H_4$ has a large optical gap at 160 nm wavelength (7.75 eV) in the ultraviolet (UV) region, but after introducing Au atoms the optical gaps of clusters $Au_n(SiO_2)_4O_2H_{4-n}$ ($n = 1-4$) reduce to 463∼485 nm (around 2.6 eV) in the visible region as illustrated in Table 1. It is obvious that the introduction of Au atoms significantly modifies the optical properties of the original cluster. More details on the absorption properties of these Au_1-adsorbed clusters are listed in Table 1 and depicted in Figure 3. For all these clusters, the lowest two absorption bands are located in the visible region 400∼500 nm (2.5∼3.1 eV), which are approximate to the experimental results of Au atoms deposited on amorphous silica (2.48 and 2.75 eV).[19] The strongest photon

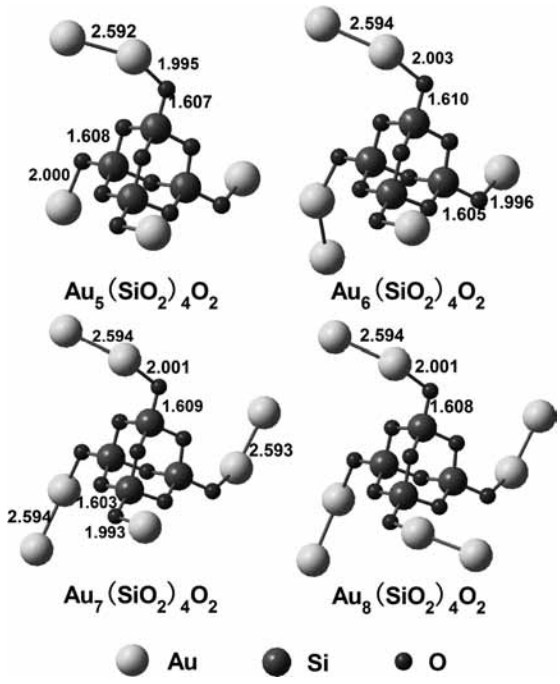

Figure 5. Ground-state structures of Au_2-adsorbed clusters $Au_n(SiO_2)_4O_2$ ($n = 5-8$). Calculated bond lengths are given in angstroms.

absorptions of these clusters are observed within a narrow range from 428 to 440 nm (second peaks of all lines in Figure 3). As the Au atoms increase from 1 to 4, only very small red shifts occur on the absorption maxima of clusters $Au_n(SiO_2)_4O_2H_{4-n}$, which indicates that the wavelengths are insensitive to the number of Au atoms. However, the absorption intensities of the visible light increase almost linearly with increasing the Au atoms, so for $Au_4(SiO_2)_4O_2$ the molar absorbance of the visible light is about four times greater than $Au(SiO_2)_4O_2H_3$, and the highest absorption is at 440 nm.

From the excitation calculations, we conclude that the visible absorption of Au_1-adsorbed clusters $Au_n(SiO_2)_4O_2H_{4-n}$ ($n = 1-4$) originates from the Au−O interaction. Taking the case of closed-shell system $Au(SiO_2)_4O_2H_3$, the maximum absorption at 428 nm is predominantly due to the electronic transition from the highest occupied molecular orbital (HOMO) to the lowest unoccupied molecular orbital (LUMO) with the transition coefficient up to 0.64, which is accompanied by the weak electronic charge transfer from the inner O atom to the outer Au atom as illustrated by the molecular orbital diagram in Figure 4. For other $Au_n(SiO_2)_4O_2H_{4-n}$ clusters, charge transfers also occur in the AuO radicals, resulting in the strong visible light absorptions, despite that the increased AuO radicals induce degenerate electronic orbitals and then more complicated electronic transitions. Therefore, electronic charge transfer between Au and the neighboring O atoms is the main mechanism to induce the visible absorption for Au_1-adsorbed shell-like clusters. It should be stated that TD-DFT will underestimate the excitation energies for long-range charge-transfer states, particularly in the framework of pure exchange-correlation functionals. However, for these shell-like clusters the excited charge transfers are weak and short-range, and the adopted hybrid functional containing partial exact exchange potential can lower the inaccuracy more or less. In addition, here we focused our interest in the absorption ranges and the optical tunabilities. As a result, it could be clearly concluded that the AuO radicals play key roles in the visible absorptions for the Au_1-adsorbed shell-like clusters, and this also elucidates the agreements between our calculation results and experimental measurements on silica surface.[19] Because there are only tiny structural differences of the AuO radicals, the absorption intensities of these clusters increase linearly with the number of Au atoms while little red shifts of the absorption spectra take place. For $Au_4(SiO_2)_4O_2$ with S_4 point-group symmetry in particular, the four equivalent AuO radicals make its absorption the strongest among this group of clusters.

2. Clusters Containing Au Dimers at Terminals ($n = 5-8$). By adding more gold atoms to the terminals of the cluster $Au_4(SiO_2)_4O_2$, the Au_2-adsorbed group of shell-like clusters are formed. These clusters are denoted as $Au_n(SiO_2)_4O_2$ ($n = 5-8$) for 1 to 4 Au_2 dimers being attached, respectively. Owing to the function of Au_2 dimers, the optical properties of the clusters are expected to be distinct from the previous group. Differently from the first group, the terminal Au atoms of the dimers in these clusters are not fully electronic spin-paired. As a result, the ground-state spin multiplicities of the Au_2-adsorbed clusters are doublet, triplet, quartet, and quintet, respectively, for different n. Figure 5 shows their ground-state structures. Similarly to the first group, there are only small changes in the bond lengths and bond angles of the clusters for different n, and particularly the cluster core $(SiO_2)_4O_2$ still approximately keeps T_d point-group symmetry. The similar results of both groups demonstrate the high stability of the core $(SiO_2)_4O_2$. In the Au_2-adsorbed group, the Au−Au bond lengths are about 2.594 Å, which is a little larger than our computed bond length 2.560 Å of the diatomic molecule Au_2 in the same theoretical level. Similarly to the Au−O bonds in the first group, the electron-cloud densities of Au−Au bonds decrease when the inner Au atoms offer partial electrons to form covalent bonds with O atoms, resulting in the small extensions of Au−Au bonds in these clusters compared with the Au_2 molecule. All the Au−Au−O bond angles are around 146°, and the corresponding Au−O−Si bond angles are within 120∼125° which are larger than those of the Au_1-adsorbed clusters. Nevertheless, the Au−O−Si bond angles of the other dangling AuO radicals still maintain around 115°, and the AuO bond lengths of both Au_2O and Au_1O types in these clusters also keep about 2.000 Å. It means that before all Au_1-type adsorbates convert to Au_2-type ones, such as for $n = 5$, 6, and 7, the absorption spectra of these clusters should also have the same maxima in some regions as the Au_1-adsorbed clusters exhibit.

After forming Au_2 dimers, the optical gaps of these clusters further reduce to about 1600 nm in the infrared region. Table 2 lists the optical gaps of this class of clusters as well as other significant excited transitions, and the absorption properties are plotted in Figure 6. Compared with the first group of clusters (blue dotted line in Figure 6), besides the same absorption at around 440 nm resulting from the Au_1O radicals while n is less than 8 as we expected, three additional absorption maxima appear in the NIR region. In other words, the absorption spectra exhibit a great extension from the visible to the NIR region while Au_2 dimers are introduced. More interestingly, red shifts were also observed in the gold growing process of semicontinuous nanoshell,[10] although they may originate from a mechanism different to these small clusters. Among the three newly emerging peaks, the two located within 600∼800 nm (1.7∼2.1 eV) are so weak that they are not listed in Table 2, and the remarkable one within 900∼1200 nm is relatively stronger which may satisfy the NIR absorption condition for tumors thermal therapy. Although the former two are very weak in intensity, they are in agreement with the experimental measure-

TABLE 2: Calculated Excitation Energies (E, eV), Wavelengths (λ, nm) and Corresponding Oscillator Strengths (f) of $Au_n(SiO_2)_4O_2$ ($n = 5-8$) Clusters in Two Dominant Absorption Regions[a]

	$Au_5(SiO_2)_4O_2$			$Au_6(SiO_2)_4O_2$			$Au_7(SiO_2)_4O_2$			$Au_8(SiO_2)_4O_2$		
range	E	λ	$f \times 100$	E	λ	$f \times 100$	E	λ	$f \times 100$	E	λ	$f \times 100$
optical gap	0.76	1639.5	0.04	0.77	1608.7	0.08	0.78	1589.0	0.09	0.79	1578.2	0.14
1000−1100 nm	1.15	1079.0	0.95	1.14	1086.7	3.44	1.15	1080.0	3.09	1.15	1081.4	2.45
				1.15	1076.1	1.28	1.15	1077.3	3.83	1.15	1078.4	4.02
							1.17	1060.0	0.67	1.15	1078.4	4.02
	1.23	1008.3	2.23	1.21	1027.5	0.57	1.21	1024.3	0.91	1.21	1023.2	0.63
				1.22	1015.5	1.09	1.21	1022.9	1.04	1.21	1023.1	1.09
							1.22	1019.9	0.35	1.21	1023.1	1.09
400−500 nm[b]	2.54	487.7	0.91	2.53	491.1	1.30	2.54	488.0	1.87	2.54	487.3	2.19
				2.54	489.0	1.29	2.54	487.6	1.22	2.55	487.2	1.29
										2.55	487.2	1.29
							2.71	457.3	1.01	2.73	453.7	1.84
							2.72	455.4	1.25	2.73	453.7	1.84
							2.73	454.7	0.98	2.74	453.2	1.69
	2.82	439.6	2.11	2.83	437.7	4.95	2.84	436.9	3.35			
	2.83	438.1	4.54	2.85	435.7	2.24						
	2.83	437.8	4.27									

[a] The first row gives the optical gaps of these clusters. [b] Only significant transitions ($f \times 100 \geq 0.9$) are listed for this region.

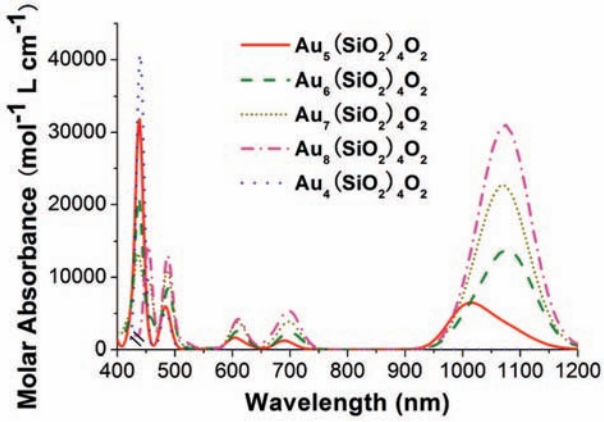

Figure 6. Absorption spectra of clusters $Au_n(SiO_2)_4O_2$ ($n = 5-8$) calculated with TDDFT/B3PW91 method. The spectra are broadened with a Gaussian type of width 0.1 eV. The blue dotted line represents the result of $Au_4(SiO_2)_4O_2$ for comparison.

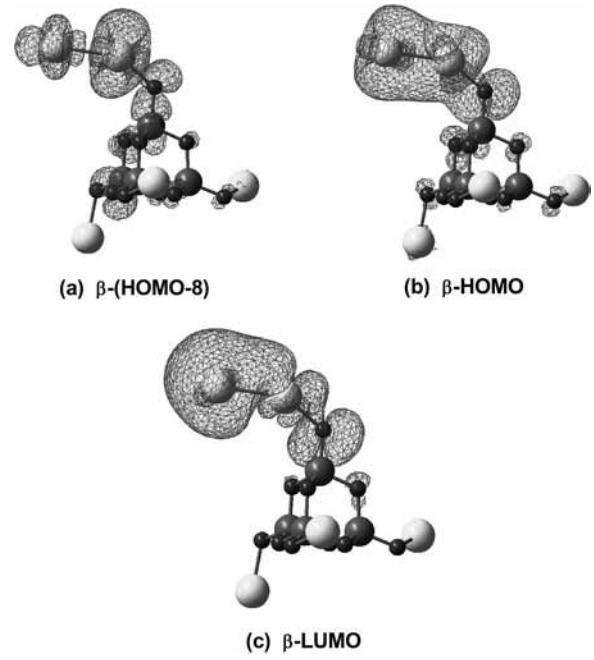

Figure 7. The β-(HOMO-8), β-HOMO, and β-LUMO orbitals of the cluster $Au_5(SiO_2)_4O_2$.

ments of Au_2 dimers deposited on amorphous silica (1.88 and 2.15 eV),[20] providing the reliability of the theoretical method used for these Au_2-adsorbed clusters. The intensities of these three peaks rise proportionally with increasing the dimers, which indicates that the Au_2 dimers make contributions to these absorptions, while the intensity of another peak at about 440 nm weakens as expected because of the reduction of the Au_1O radicals. Similarly to the case of $Au_4(SiO_2)_4O_2$, the cluster $Au_8(SiO_2)_4O_2$ is also with S_4 point-group symmetry and the four equivalent Au_2 dimers induce significantly strong absorption of NIR light. Furthermore, from the viewpoint of electronic structure, the exited transitions at 900∼1200 nm of open-shell system $Au_5(SiO_2)_4O_2$ mainly come from the electronic transitions from β-HOMO and β-(HOMO-8) to β-LUMO with the transition coefficients up to 0.65 and 0.59 respectively, associated with the weak charge transfer from the inner gold atom to the neighboring outer one as shown in Figure 7. For $n > 5$, charge transfer between the two Au atoms of Au_2 dimers is also the mechanism for the appearance of the intense NIR absorption, although the electronic orbital transitions are more complicated than $Au_5(SiO_2)_4O_2$. As a result, we concluded that Au−Au interactions make the most contributions to the NIR absorptions for these Au_2-adsorbed shell-like clusters. Also, since Au_1- and Au_2-adsorbed clusters could be regarded as single-shell and two-shell coating cases, respectively, for the latter the Au−Au interactions could consequently be considered as the interaction between the inner shell and the outer shell, somewhat analogous to the nanoshells.

From Au_1- to Au_2-adsorbed clusters, the wavelengths of intense absorption vary obviously from the visible to the NIR region. However, in each group the number of major contributing adsorbate, that is, Au atom in the first case or Au_2 dimer in the second one, does not affect the absorption wavelength dramatically, but only changes the absorption intensity, as shown in Figures 3 and 6. These features suggest effective and definite spectra tunability could be implemented on the Au-adsorbed shell-like clusters. In addition, the outstanding stability of the core $(SiO_2)_4O_2$ demonstrates more advantages in the preparation of such new cluster materials.

Conclusions

In this work, by using the static and time-dependent DFT approach, we constructed two groups of Au-adsorbed shell-like

clusters, $Au_n(SiO_2)_4O_2H_{4-n}$ ($n = 1-4$) and $Au_n(SiO_2)_4O_2$ ($n = 5-8$), and studied how their optical properties are influenced by the types and the number of gold fragments adsorbed to the core $(SiO_2)_4O_2$. The clusters are in molecular scale analogous to the semicontinuous nanoshells and could be obtained in experiment from the results that gold atoms tend to bind with dangling oxygen defects while they are deposited on silica surface.[19,20] Our calculations show that the core $(SiO_2)_4O_2$ of all shell-like clusters keeps a stable tetrahedral configuration with T_d point-group symmetry, and for $n = 4$ and 8 the structures of entire cluster possess S_4 point-group symmetry, which is the same as the magic number cluster $(SiO_2)_4O_2H_4$. The structural stability of the oxy-silica cluster $(SiO_2)_4O_2$ implies possibilities to use it as a core to build relevant compounds and cluster materials such as these Au-adsorbed shell-like clusters we considered.

Because of the weak electronic charge transfers within AuO radicals or Au_2 dimers, it has been observed that by adjusting the adsorbates over the core $(SiO_2)_4O_2$, we can tune the absorption wavelengths of the clusters from the UV−visible region to the NIR region. Among each cluster group, Au_1- or Au_2-adsorbed clusters, the number of adsorbates only affects the absorption intensities while the adsorbates type determines the absorption wavelengths. The definite variations of spectra related to the types and the number of adsorbates demonstrate that the highly stable oxy-silica core $(SiO_2)_4O_2$ has advantages for preparing novel cluster materials with easily controlled tunable optical properties.

In addition, for our target shell-like clusters, the absorption intensities can be augmented rapidly by increasing the number of gold atoms or dimers. As a result, $Au_4(SiO_2)_4O_2$ and $Au_8(SiO_2)_4O_2$ exhibit the strongest absorption of visible light at 400∼500 nm and NIR light at 900∼1200 nm respectively, and the latter meets the requirement of being a nanobullet of molecular size for killing tumor cells. Therefore, associated with the continuous progress of synthesis techniques, it is promising to consider such Au-adsorbed shell-like clusters for tumors thermal therapy.

Acknowledgment. The authors are grateful to Professor Yufen Li for useful discussions and acknowledge Professor Wenning Wang and Professor Kangnian Fan for their help in the computational calculations. This work is supported by Chinese NSF (Grant 10004002). Some of the calculations were performed at the National High Performance Computing Center of Fudan University and Shanghai Supercomputing Center.

Supporting Information Available: Optimized geometric structures for $(SiO_2)_4O_2H_4$, $Au_4(SiO_2)_4O_2$, and $Au_8(SiO_2)_4O_2$ with S_4 configurations, and detailed information about the weak absorption within 600∼800 nm for Au_2-adsorbed clusters $Au_n(SiO_2)_4O_2$ ($n = 5-8$). This material is available free of charge via the Internet at http://pubs.acs.org.

References and Notes

(1) Jain, P. K.; El-Sayed, I. H.; El-Sayed, M. A. *Nanotoday* **2007**, *2*, 18.

(2) Connor, E. E.; Mwamuka, J.; Gole, A.; Murphy, C. J.; Wyatt, M. D. *Small* **2005**, *1*, 325.

(3) El-Sayed, I. H.; Huang, X.; El-Sayed, M. A. *Cancer Lett.* **2006**, *239*, 129.

(4) Link, S.; El-Sayed, M. A. *J. Phys. Chem. B* **1999**, *103*, 4212.

(5) Huang, X.; El-Sayed, I. H.; Qian, W.; El-Sayed, M. A. *J. Am. Chem. Soc.* **2006**, *128*, 2115.

(6) Hirsch, L. R.; Stafford, R. J.; Bankson, J. A.; Sershen, S. R.; Rivera, B.; Price, R. E.; Hazle, J. D.; Halas, N. J.; West, J. L. *Proc. Natl. Acad. Sci. U.S.A.* **2003**, *100*, 13549.

(7) Loo, C.; Lowery, A.; Halas, N.; West, J.; Drezek, R. *Nano Lett.* **2005**, *5*, 709.

(8) Tromberg, B. J.; Shah, N.; Lanning, R.; Cerussi, A.; Espinoza, J.; Pham, T.; Svaasand, L.; Butler, J. *Neoplasia* **2000**, *2*, 26.

(9) Weissleder, R. *Nat. Biotechnol.* **2001**, *19*, 316.

(10) Oldenburg, S. J.; Averitt, R. D.; Westcott, S. L.; Halas, N. J. *Chem. Phys. Lett.* **1998**, *288*, 243.

(11) Prodan, E.; Radloff, C.; Halas, N. J.; Nordlander, P. *Science* **2003**, *302*, 419.

(12) Hobbs, S. K.; Monsky, W. L.; Yuan, F.; Roberts, W. G.; Griffith, L.; Torchilin, V. P.; Jain, R. K. *Proc. Natl. Acad. Sci. U.S.A.* **1998**, *95*, 4607.

(13) Sun, Q.; Wang, Q.; Rao, B. K.; Jena, P. *Phys. Rev. Lett.* **2004**, *93*, 186803. (a) Sun, Q.; Wang, Q.; Rao, B. K.; Jena, P. *Phys. Rev. Lett.* **2005**, *94*, 049901.

(14) Zhao, G.; Zhi, L.; Guo, L.; Zeng, Z. *J. Chem. Phys.* **2007**, *127*, 234705.

(15) Xie, R. H.; Bryant, G. W.; Sun, G.; Kar, T.; Chen, Z.; Smith, V. H., Jr.; Araki, Y.; Tagmatarchis, N.; Shinohara, H.; Ito, O. *Phys. Rev. B* **2004**, *69*, 201403.

(16) Xie, R. H.; Bryant, G. W.; Zhao, J.; Kar, T.; Smith, V. H. *Phys. Rev. B* **2005**, *71*, 125422.

(17) Xu, C.; Wang, W.; Zhang, W.; Zhuang, J.; Liu, L.; Kong, Q.; Zhao, L.; Long, Y.; Fan, K.; Qian, S.; Li, Y. *J. Phys. Chem. A* **2000**, *104*, 9518.

(18) Kong, Q.; Zhao, L.; Wang, W.; Wang, C.; Xu, C.; Zhang, W.; Liu, L.; Fan, K.; Li, Y.; Zhuang, J. *J. Comput. Chem.* **2005**, *26*, 584.

(19) Antonietti, J. M.; Michalski, M.; Heiz, U.; Jones, H.; Lim, K. H.; Rösch, N.; Del Vitto, A.; Pacchioni, G. *Phys. Rev. Lett.* **2005**, *94*, 213402.

(20) Del Vitto, A.; Pacchioni, G.; Lim, K. H.; Rösch, N.; Antonietti, J.; Michalski, M.; Heiz, U.; Jones, H. *J. Phys. Chem. B* **2005**, *109*, 19876.

(21) Wu, K.; Li, J.; Lin, C. *Chem. Phys. Lett.* **2004**, *388*, 353.

(22) Öğüt, S.; Idrobo, J. C.; Jellinek, J.; Wang, J. *J. Clust. Sci.* **2006**, *17*, 609.

(23) Stener, M.; Nardelli, A.; De Francesco, R.; Fronzoni, G. *J. Phys. Chem. C* **2007**, *111*, 11862.

(24) Frisch, M. J. ; Trucks, G. W.; Schlegel, H. B.; Scuseria, G. E.; Robb, M. A.; Cheeseman, J. R.; Montgomery, J. A., Jr.; Vreven, T.; Kudin, K. N.; Burant, J. C.; Millam, J. M.; Iyengar, S. S.; Tomasi, J.; Barone, V.; Mennucci, B.; Cossi, M.; Scalmani, G.; Rega, N.; Petersson, G. A.; Nakatsuji, H.; Hada, M.; Ehara, M.; Toyota, K.; Fukuda, R.; Hasegawa, J.; Ishida, M.; Nakajima, T.; Honda, Y.; Kitao, O.; Nakai, H.; Klene, M.; Li, X.; Knox, J. E.; Hratchian, H. P.; Cross, J. B.; Adamo, C.; Jaramillo, J.; Gomperts, R.; Stratmann, R. E.; Yazyev, O.; Austin, A. J. Cammi, R.; Pomelli, C.; Ochterski, J. W.; Ayala, P. Y.; Morokuma, K.; Voth, G. A.; Salvador, P.; Dannenberg, J. J.; Zakrzewski, V. G.; Dapprich, S.; Daniels, A. D.; Strain, M. C.; Farkas, O.; Malick, D. K.; Rabuck, A. D.; Raghavachari, K.; Foresman, J. B.; Ortiz, J. V.; Cui, Q.; Baboul, A. G.; Clifford, S.; Cioslowski, J.; Stefanov, B. B.; Liu, G.; Liashenko, A.; Piskorz, P.; Komaromi, I.; Martin, R. L.; Fox, D. J.; Keith, T.; Al-Laham, M. A.; Peng, C. Y.; Nanayakkara, A.; Challacombe, M.; Gill, P. M. W.; Johnson, B.; Chen, W.; Wong, M. W.; Gonzalez, C.; Pople, J. A. *Gaussian 03*, revision B.05; Gaussian, Inc.: Pittsburgh, PA, 2003.

(25) Gorelsky, S. I. *SWizard program*, revision 4.5; http://www.sg-chem.net/.

(26) O'Brien, L. C.; Oberlink, A. E.; Roos, B. O. *J. Phys. Chem. A* **2006**, *110*, 11954.

(27) Schwerdtfeger, P.; Dolg, M.; Schwarz, W. H. E.; Bowmaker, G. A.; Boyd, P. D. W. *J. Chem. Phys.* **1989**, *91*, 1762.

(28) Zanella, R.; Sandoval, A.; Santiago, P.; Basiuk, V. A.; Saniger, J. M. *J. Phys. Chem. B* **2006**, *110*, 8559.

(29) Ichino, T.; Gianola, A. J.; Andrews, D. H.; Lineberger, W. C. *J. Phys. Chem. A* **2004**, *108*, 11307.

(30) Okabayashi, T.; Koto, F.; Tsukamoto, K.; Yamazaki, E.; Tanimoto, M. *Chem. Phys. Lett.* **2005**, *403*, 223.

JP811347C